Clays and Clay Minerals, Vol. 47, No. 3, 338–347, 1999.

STRUCTURAL STUDY OF MONOMETHYLAMMONIUM AND DIMETHYLAMMONIUM-EXCHANGED VERMICULITES

A. VAHEDI-FARIDI AND STEPHEN GUGGENHEIM

Department of Earth and Environmental Sciences, University of Illinois at Chicago, 845 W. Taylor St., Chicago, Illinois 60607, USA

Abstract—Vermiculite crystals from Santa Olalla, Spain, were first Na exchanged and then intercalated with monomethylammonium (= $NH_3(CH_3)^+$, MMA) and dimethylammonium (= $NH_2(CH_3)_2^+$, DMA) molecules, respectively, by immersion in 1 M ammonium-chloride solutions at 65°C for 2–3 wk. MMA- and DMA-exchange with vermiculite resulted in crystals with near perfect three-dimensional stacking, suitable for single crystal X-ray diffraction analysis. Unit cell parameters are: a = 5.353(2) Å, b = 9.273(3) Å, c = 11.950(6) Å, and β = 98.45(4)° for MMA-exchanged vermiculite and a = 5.351(2) Å, b = 9.268(4) Å, c = 12.423(8) Å, and β = 98.33(5)° for DMA-exchanged vermiculite. Refinement results are R = 0.059 and wR = 0.073 (MMA-exchanged vermiculite) and R = 0.059 and wR = 0.064 (DMA-exchanged vermiculite). The results are based on structures which show substitutional disorder, and thus the presented models are derived from average structures.

There are two distinct sites for the MMA molecule in MMA-exchanged vermiculite. One crystallographically unique MMA is oriented such that the N–C axis of the molecule is perpendicular to the basal oxygen plane, with the N ion offset from the center of the interlayer by 1.04 Å. The other MMA is located such that the N ion is at the center of the interlayer between adjacent 2:1 layers, presumably with the N–C axis of the molecule oriented parallel to the basal oxygen plane. This represents the first known occurrence of an organic molecule located exactly between the two adjacent 2:1 layers. Both sites are located between hexagonal cavities of adjacent layers. DMA molecules in DMA-exchanged vermiculite are located such that the N ion is offset from the central plane in the interlayer by 0.95 Å. A static model is proposed with two orientations of DMA to produce a DMA "zigzag" orientation of molecules parallel to the (001) plane. The plane defined by the C–N–C atoms in the molecule is perpendicular to the (001) plane. An alternate model is more dynamic, and it involves the rotation of DMA molecules about one C–N axis.

Identical starting material was used in previous studies on tetramethylammonium (TMA)-exchanged vermiculite and tetramethylphosphonium (TMP)-exchanged vermiculite. The effect of onium-ion substitutions on the 2:1 layer shows that the tetrahedral rotation angle, α, is significantly smaller for MMA- and DMA-exchanged vermiculite *vs.* TMA and TMP-exchanged vermiculite. Tetrahedral and octahedral bond distances of the 2:1 layer of the TMA, TMP, MMA, and DMA-exchanged structures may be explained by the location of the organic cation relative to the basal oxygen atom plane and by the differences in the geometries of the organic molecule. Thus, the 2:1 layer is affected by the interlayer molecule, and the 2:1 layer is not a rigid substrate, but interacts significantly with the onium ions.

Key Words—Dimethylammonium-Exchanged Vermiculite, Monomethylammonium-Exchanged Vermiculite, Organoclay, Tetramethylammonium-Exchanged Vermiculite, Tetramethylphosphonium-Exchanged Vermiculite, Vermiculite, X-ray Diffraction.

INTRODUCTION

Clays interact with many organic compounds to form complexes of varying stabilities and properties. One relatively new class of nanocomposite materials involves the pillaring of organic molecules, where these molecules prop open the silicate layers of the clays to produce a high-surface area material with fixed characteristics. These phases, or "pillared clays", are potentially useful as catalysts, adsorbents, molecular sieves, gelling agents, sensors, *etc.* Unfortunately, by the very nature of the clays used as substrates for the pillars, the materials are difficult to characterize, because most clays capable of being pillared lack three-dimensional periodicity, are fine-grained, and are usually a mixture of several phases. Spectroscopic techniques are often used to obtain data about the pillared clay and adsorbed molecules, but these techniques suffer from the inability to provide the precise topology of the atomic environment about the adsorbed molecule.

Early workers (*e.g.*, Barrer and Macleod, 1955) found that tetramethylammonium (= $N(CH_3)_4^+$, TMA) and tetraethylammonium (= $N(C_2H_5)_4^+$, TEA) intercalated in montmorillonite changed its adsorption properties. In contrast to the original montmorillonite, aliphatic and aromatic (*i.e.*, nonpolar) organic molecules, as well as polar organic species, are readily adsorbed onto the interlayer (Barrer and Millington, 1967) of TMA or TEA-exchanged montmorillonite. Although long chain alkyl ammonium cations do not produce well defined nanopores, organic cations that are small and do not fill the entire interlamellar space, such as TMA, TEA, monomethylammonium (= $NH_3(CH_3)^+$, MMA), dimethylammonium (= $NH_2(CH_3)_2^+$, DMA), trimethylammonium (= $NH(CH_3)_3^+$, TrMA), or tetra-

methylphosphonium (= $P(CH_3)_4^+$, TMP), produce interlayer cavities (sometimes referred to as a "gallery" site) with adjoining nanopore surfaces consisting of the surface of the organic molecule and the siloxane surface of the 2:1 layer. Barrer (1989) showed that the sorption characteristics of pillared clays are determined by the shape, size and, in some cases, the charge of the organic cation.

Research to determine the crystal structures of a series of related pillared clays was not attempted previously, primarily because of the lack of three-dimensional periodicity in most expandable phyllosilicate structures. However, Slade and Stone (1984) demonstrated the possibility of obtaining a three-dimensionally ordered structure of an organo-vermiculite-complex by intercalating vermiculite from Llano, Texas with aniline. We recently showed (Vahedi-Faridi and Guggenheim, 1997, 1999) that it is possible to produce an intercalated three-dimensionally periodic crystal for single crystal X-ray methods with appropriate starting material and techniques, even for pillared intercalations of spherically-charged organic cations. This study uses high-crystallinity vermiculite from Santa Olalla, Spain, to produce pillared clays by intercalating a series of organic pillars with different size and shape. Previously, Vahedi-Faridi and Guggenheim (1997, 1999) intercalated TMA and TMP pillars to compare the effects of two structures with tetrahedral pillar geometry. In this study we examine a series of increasingly complex pillars: linear (MMA), planar (DMA), and a cation with a non-planar, trigonal geometry (TrMA).

Barrer and Reay (1957) related the d(001)-value of MMA-montmorillonite (12.0 Å) to the calculated MMA heights for orientations with the N–C axis of the molecule parallel and perpendicular to the basal oxygen atom plane. They concluded that MMA assumes an orientation in MMA-montmorillonite such that the N–C axis of the molecule is not parallel to the (001) plane. Diamond and Kinter (1961) determined from an experimental cross-sectional area study of MMA-montmorillonite that the amines are oriented perpendicular to the basal oxygen atom plane. Rowland and Weiss (1961) showed that different loading of MMA on montmorillonite produced different d(001)-values. Adsorption values of near 100% cation exchange capacity (CEC) produced a d(001)-value of 11.7 Å, whereas adsorption between 300–600% CEC showed a d(001)-value of 12.4–12.9 Å, and adsorption in excess of 600% CEC exhibited basal spacings of 17.4 Å. They showed also that these phases were relatively unstable, since washing each phase with H_2O returned $c\sin\beta$ to 11.7 Å. Thus, they concluded that the amount adsorbed in excess of CEC is more loosely bound "free" amine. With a paucity of X-ray data, they concluded that the 11.7 Å phase consisted of one amine layer and that each molecule was oriented in the same direction. Williams *et al.* (1996), in a one-dimensional Fourier analysis involving neutron diffraction data (30 reflections) on a hydrated phase of MMA-vermiculite [$d(00l)$ = 12.3 Å], found a maximum in scattering densities at z = 0.5 and z = 0.415. They attributed the latter to the nitrogen of the ammonium-group, whereas the former was interpreted as interlayer water.

Rowland and Weiss (1961) intercalated montmorillonite with DMA, which resulted in a d(001)-value of 12.5 Å at 100% CEC. At concentrations between 100–400% CEC the d(001)-value was 12.7 Å, and above 600% they found a second layer of DMA forming to produce a d(001)-value of 17 Å. They suggested that DMA molecules for the 12.5 Å phase are arranged as a zigzag chain of DMA parallel to the (001) plane, whereas for the 12.7 Å phase, they believed that the cation was perpendicular to the basal oxygen atom plane. Diamond and Kinter (1961) examined hydrated *vs.* dehydrated DMA-montmorillonite with d(001)-values of 12.94 Å and 12.52 Å, respectively (*cf.*, to those of Theng *et al.* (1967) of 12.9 Å and 12.72 Å). Diamond and Kinter (1961) suggested a structure in which one of the methyl-groups of DMA is embedded into the silicate ring of the 2:1 layer, with the nitrogen ion positioned above the hole and the second methyl-group offset to maintain the appropriate C–N–C bond angle.

In this study, we compare the structures of DMA and MMA-exchanged vermiculites to previously determined vermiculite structures containing TMA and TMP (Vahedi-Faridi and Guggenheim, 1997, 1999). Each study, including the current study, used fragments from the same homogeneous vermiculite crystal, which allows precise comparisons.

EXPERIMENTAL AND RESULTS

Material and sample preparation

The vermiculite is from a weathered pyroxenite deposit (Luque *et al.*, 1985) at Santa Olalla, Spain. The structural formula (Norrish, 1973), based on 22 oxygens and anhydrous conditions, is $Ca_{0.85}(Si_{5.48},Al_{2.52})(Mg_{5.05}Ti_{0.03}Mn_{0.01}Fe^{3+}_{0.58}Al_{0.28})O_{22}$. The macroscopic crystals were cut by surgical blade to flakes of ~0.7 × 0.7 × 0.05 mm before being sodium exchanged at 80°C in a 1 M NaCl solution. Solutions were renewed every second day and the exchange rate of the crystals analyzed (CuKα radiation) with a Siemens D-5000 X-ray powder diffractometer. The exchange-product has d(001) of 11.9 Å, consistent with a "monolayer" phase of Na-vermiculite (de la Calle *et al.*, 1985). The Na-vermiculite flakes were subsequently treated with 1 M solutions of MMA, DMA, and TrMA-chloride, respectively, at 65°C for 2–3 wk. Individual flakes were examined on the powder diffractometer to check the exchange process and the solutions changed every

https://doi.org/10.1346/CCMN.1999.0470310 Published online by Cambridge University Press

Table 1. Atomic coordinates of MMA-vermiculite.

Site	*x*	*y*	*z*	[1]K	[2]U_{11}	U_{22}	U_{33}	U_{23}	U_{13}	U_{12}	U_{eq}
M(1)	0.5	0	0	0.25	0.010(1)	0.003(1)	0.046(2)	0	0.006(1)	0	0.0198(9)
M(2)	0	0.1686(2)	0	0.5	0.0102(9)	0.0019(8)	0.047(1)	0	0.0061(9)	0	0.0196(7)
T	0.4095(3)	0.1667(2)	0.2308(2)	1.0	0.0103(6)	0.0021(5)	0.044(1)	0.0000(7)	0.0053(6)	0.0000(5)	0.0187(5)
O(1)	0.456(1)	0	0.2807(6)	0.491(3)	0.026(2)	0.008(2)	0.045(3)	0	0.005(2)	0	0.026(1)
O(2)	0.1601(8)	0.2344(5)	0.2799(5)	0.987(3)	0.021(2)	0.016(2)	0.054(3)	0.003(2)	0.008(2)	0.005(2)	0.030(1)
O(3)	0.3632(7)	0.1666(4)	0.0924(4)	1.0	0.010(1)	0.005(1)	0.050(2)	0.001(2)	0.008(2)	0.001(1)	0.021(1)
OH	0.352(1)	0.5	0.0870(6)	0.5	0.016(2)	0.008(2)	0.061(3)	0	0.007(2)	0	0.028(1)
N(1)	0	0	0.5	0.253(3)	0.189(3)	0.173(3)	0.143(3)	0	0.016(3)	0	0.169(2)
N(2)	0.969(3)	0	0.413(3)	0.275(3)	0.141(3)	0.137(3)	0.133(3)	0	0.014(3)	0	0.138(2)
C	0.93	0	0.535	0	0	0	0	0	0	0	0

[1] K = refined value of site occupancy, except where noted in text.

[2] Note: Displacement parameters are of the form $\exp[-2\pi^2(U_{11}h^2a^{*2} + U_{22}k^2b^{*2} + U_{33}l^2c^{*2} + 2U_{12}hka^*b^* + 2U_{13}hla^*c^* + 2U_{23}klb^*c^*)]$.

other day. The observation of a unique set of spacings along $c\text{Sin}\beta$ occurred in ~95% of the samples [$d(001)$ = 12.13 Å for MMA-vermiculite, $d(001)$ = 12.48 Å for DMA-vermiculite, and $d(001)$ = 12.93 Å for TrMA-vermiculite] which indicated complete exchange. However, because flakes were dried under normal laboratory conditions, these phases are not dehydrated.

Single crystal X-ray data collection

Buerger precession photographs of the majority of the examined MMA- and DMA-vermiculite crystals showed a high degree of three-dimensional ordering as illustrated by sharp $k \neq 3n$ type reflections. In contrast, the unexchanged-vermiculite and the TrMA-vermiculite showed streaking along the [001]* direction for $k \neq 3n$ reflections indicating a high degree of stacking disorder. Space group *C*2/*m* was chosen for the refinement of MMA and DMA-exchanged vermiculite due to the systematic presence of $h + k = 2n$ reflections, and an apparent mirror plane perpendicular to a two-fold axis. The best crystal from each batch of MMA-vermiculite and DMA-vermiculite crystals was mounted on a Picker four-circle diffractometer. Unit cell dimensions (MoKα = 0.71069 Å) were obtained from 19 unique reflections from 8 octants (to yield 8 × 19 = 152 reflections). The results were: a = 5.353(2) Å, b = 9.273(3) Å, c = 11.950(6) Å, and β = 98.45(4)° for MMA-vermiculite and a = 5.351(2) Å, b = 9.268(4) Å, c = 12.423(8) Å, and β = 98.33(5)° for DMA-vermiculite.

Data were collected from half the limiting sphere for 2θ = 4–60° with h equals −8 to 8, k equals −14 to 14 and l equals 0 to 18. Three check reflections were measured every 300 min to determine electronic and crystal stability. A total of 1791 reflections for MMA-vermiculite and 1853 reflections for DMA-vermiculite was obtained. Lorentz and polarization corrections were made and absorption corrected by the psi-scan based technique utilized by the SHELXTL PLUS program (Siemens, 1990), with 10° intervals in ψ, resulting in a total of ~400 reflections. Reflections were not used where the intensity was <6σ. After omitting these reflections and averaging the reflections based on symmetry considerations, there were 669 independent reflections for MMA-vermiculite and 725 independent reflections for DMA-vermiculite. An additional 30 (MMA-vermiculite) and 35 (DMA-vermiculite) reflections were omitted, respectively, due to unusual peak shape.

STRUCTURAL REFINEMENT

The SHELXTL PLUS program (Siemens, 1990) was used also for the refinement. Starting atomic coordinates for the silicate layer were taken from the refinement of TMA-vermiculite (Vahedi-Faridi and Guggenheim, 1997). Scattering factors were taken from Cromer and Mann (1968) and the method of Sales (1987) was used to calculate half ionized atoms or scattering factors for sites where isomorphous substitution occurs. The refinement used unit weights and a single scale factor for the reflections.

MMA-vermiculite

After initial refinement of the 2:1 layer, a Fourier map of the interlayer region revealed two independent peaks, associated with different positions of nitrogen-ions in the MMA molecule. These positions were refined and yielded site occupancy factors of 25 and 28% (Table 1). The distance of 1.03 Å between these two sites does not correlate with the N–C bond distance of 1.47 Å, indicating that these are two independent MMA sites in an average structure. We refer to the nitrogen atom positions, N(1) and N(2), when discussing the nitrogen, and MMA(1) and MMA(2) for discussions relating to the molecule associated with N(1) and N(2), respectively. In addition to the above argument, charge sums of both sites yielded a value of 0.8 electrostatic valency units (*evu*) per unit cell, which is close to the value of 0.85 *evu*/unit cell as derived by chemical analysis (Norrish, 1973). In the later stages of the refinement, a Fourier difference

Table 2. Atomic coordinates of DMA-vermiculite.

Site	*x*	*y*	*z*	[1]K	[2]U_{11}	U_{22}	U_{33}	U_{23}	U_{13}	U_{12}	U_{eq}
M(1)	0.5	0	0	0.25	0.006(1)	0.004(1)	0.043(2)	0	0.006(1)	0	0.0174(9)
M(2)	0	0.1685(2)	0	0.5	0.0065(8)	0.0029(8)	0.045(2)	0	0.0062(8)	0	0.0182(7)
T	0.4077(2)	0.1667(1)	0.2225(1)	1.0	0.0071(5)	0.0061(6)	0.040(1)	0.0002(6)	0.0055(5)	0.0004(4)	0.0176(5)
O(1)	0.452(1)	0	0.2691(6)	0.5	0.030(3)	0.013(2)	0.045(4)	0	0.003(3)	0	0.030(2)
O(2)	0.1584(7)	0.2354(5)	0.2691(4)	1.0	0.018(2)	0.024(2)	0.049(3)	0.003(2)	0.009(2)	0.009(2)	0.030(1)
O(3)	0.3612(6)	0.1663(4)	0.0873(3)	1.0	0.008(1)	0.009(1)	0.048(3)	0.002(2)	0.008(1)	0.001	0.021(1)
OH	0.3623(8)	0.5	0.0840(5)	0.5	0.011(2)	0.010(2)	0.056(4)	0	0.007(2)	0	0.025(2)
N(1)	0.477(4)	0.5	0.424(2)	0.42(1)	0.10(1)	0.16(1)	0.12(1)	0	0.022(9)	0	0.125(6)
C(1)	0.236	0	0.5	0	0	0	0	0	0	0	0
C(2)	0.823	0.077	0.5	0	0	0	0	0	0	0	0

[1] K = refined value of site occupancy, except where noted in text.
[2] Note: Displacement parameters are of the form $\exp[-2\pi^2(U_{11}h^2a^{*2} + U_{22}k^2b^{*2} + U_{33}l^2c^{*2} + 2U_{12}hka^*b^* + 2U_{13}hla^*c^* + 2U_{23}klb^*c^*)]$.

electron density (DED) map located a peak consistent with a methyl group of one of the MMA cations (0.93, 0, 0.535). The final R value, $R = \Sigma(||F_o| - |F_c||)/\Sigma|F_o|$, including anisotropic displacement factors, refined to 0.059 ($wR = 0.073$).

DMA-vermiculite

Isotropic refinement of the 2:1 layer in DMA-vermiculite resulted in an initial R value of 0.145. A DED map located a single site for the DMA cation in the interlayer region above the hexagonal cavities (Table 2). Nitrogen was placed at this site (0.477, 0, 0.42) and further isotropic refinement lowered the R factor to 0.123. A DED map showed two peaks (at $z = 0.5$) consistent with methyl-group sites. The standard deviation, s, of the DED difference Fourier peak was calculated at 0.092 e/Å^3 (Ladd and Palmer, 1977). Both peaks (0.83 and 0.87 e/Å^3) are well above 3s. Inclusion of these sites in the refinement process did not result in a further lowering of the R value. Final anisotropic refinement reduced the R value to 0.059 ($wR = 0.064$).

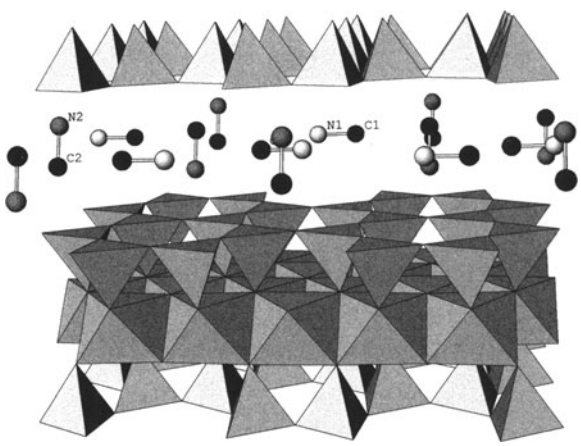

Figure 1. A model structure of MMA-exchanged vermiculite viewed nearly along the [100] direction. The MMA sites (related N and C atoms illustrated as "ball and stick") are partially-occupied as noted in the text. A complete 2:1 layer and a tetrahedral sheet from an adjacent layer are shown. Within the 2:1 layer, the polyhedral corners represent oxygen-atom centers. Octahedra represent M sites and tetrahedra represent T sites (Si, Al).

DISCUSSION

MMA-vermiculite

The intercalation of vermiculite with MMA produces a $d(001)$-value of 11.8 Å ($c\mathrm{Sin}\beta$), which is consistent with the spacings obtained by powder diffraction techniques (11.7 Å, Rowland and Weiss, 1961; 12.0 Å, Barrer and Reay, 1957) of MMA-montmorillonite for adsorption values at near 100% cation exchange. Larger basal spacings could not be achieved with Santa Olalla vermiculite, and we assume that the layer charge of the vermiculite does not allow further expansion.

Figure 1 shows the model for the distribution of MMA-cations in the interlayer of MMA-vermiculite with partial occupancy of the MMA sites (25 and 28%), and Figure 2 shows the rotational radii of the MMA molecule for two orientations. Since the distance between MMA(1) and MMA(2) is 1.03 Å, it is concluded from the rotational radii that both sites cannot be occupied in the unit cell simultaneously; thus, the observed structure is an average structure. The C–N axis of the MMA(1) molecules is perpendicular to the basal oxygen plane with the N(1) located at $z =$

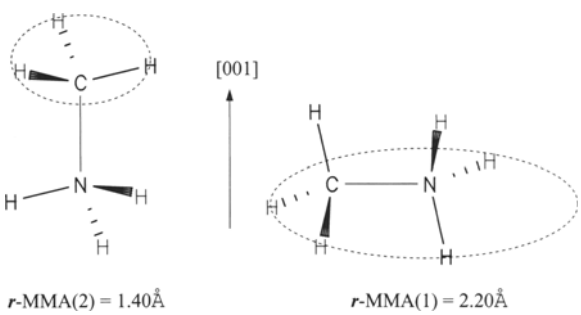

Figure 2. Rotational radii of MMA(1) and MMA(2).

https://doi.org/10.1346/CCMN.1999.0470310 Published online by Cambridge University Press

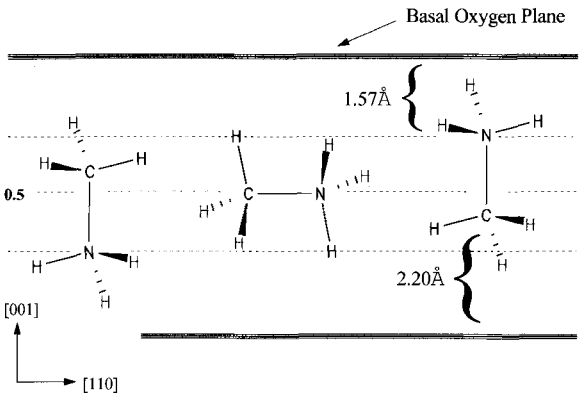

Figure 3. Local arrangement of MMA-exchanged vermiculite showing three MMA molecules along the [110] direction. In the structure, the three MMA sites cannot be occupied simultaneously.

Table 3. Single crystal pillared-vermiculite data.

	d(001)-value (RT)[1]	P,N–CH_3[2]	Pillar-height[3]	P,N–Basal-oxygen-plane[4]	P,N–Inter-layer-center[5]
TMP	14.394 Å	1.87 Å	4.68 Å	2.7 Å	1.2 Å
TMA	13.494 Å	1.47 Å	4.16 Å	1.91 Å	1.52 Å
TrMA	12.93 Å	1.47 Å	3.25–4.16 Å	—	—
DMA	12.289 Å	1.47 Å	3.25 Å	1.89 Å	0.95 Å
MMA	11.821 Å	1.47 Å	2.93 Å	1.57 Å	1.03 Å

[1] *d*(001)-value at room temperature and relative humidity.
[2] Phosphorus, Nitrogen–to methylgroup distance.
[3] Calculated minimum pillar-height for observed orientations.
[4] Phosphorus, Nitrogen–to basal oxygen plane distance.
[5] Phosphorus, Nitrogen–to center of interlayer distance.

0.413 and located above the hexagonal cavity. Figure 3 shows the C–N axis of the MMA-molecule situated perpendicular to the basal oxygen atom planes and pointing towards the lower and upper hexagonal cavities. The offset from the center of the interlayer (z = 0.5) as determined from the N ion is 1.04 Å (Table 3). The distance from the ammonium group to the oxygen atom plane is 1.57 Å, thus being considerably smaller than the distance of the methyl-group to the upper plane of basal oxygen atoms (2.20 Å). Although the methyl-group and ammonium-group are approximately equal in size, positive charge is located on the N ion of the latter. This charge interacts with the negative charge of the silicate layer, thereby requiring a shorter distance in comparison with the methyl-group to basal-oxygen plane distance; there is an electrostatic interaction between the ammonium-group and the oxygens of the hexagonal hole. For steric reasons involving the tetrahedral geometry of the TMA molecule, this interaction does not occur between TMA and the 2:1 layer in TMA-vermiculite (Vahedi-Faridi and Guggenheim, 1997), where a methyl-group is pointing towards the closest hexagonal cavity. Although the structure is a "one-layer" structure where there is a single plane of interlayer pillars, there is a random alternation between MMA-pillars associated with the lower plane and the upper plane (Figure 3).

A second MMA molecule occurs at the N(2) site at z = 0.5, between adjacent hexagonal cavities across the interlayer. In contrast to MMA(1), there is no residual electron density in a DED map to locate the associated methyl-group, and we have no direct evidence regarding its location. A keying of the methyl-group into the hexagonal cavities, however, would result in a much smaller distance of the methyl-group to (basal) oxygen atom plane than that of the ammonium-group to the oxygen atom plane. As noted above, electrostatic interactions would not require such an arrangement. Thus, a more likely model is that the molecule is dynamic and is oriented parallel or nearly parallel to the basal oxygen atom planes (as shown in Figures 1 and 3). It is noteworthy that the N(2) site is located exactly between two silicate layers, since all other organoclay structures refined to date show the source of the charge in the (organic) molecule more closely associated with a 2:1 layer.

Williams *et al.* (1996) reported a neutron diffraction study on the hydrated phase of MMA-vermiculite ($d(00l)$ = 12.3 Å). The one-dimensional analyses showed a maximum in scattering densities at z = 0.5 and z = 0.415. They attributed the latter to the N of the ammonium-group, as found here. The peak at z = 0.5 was thought to be interlayer water of the hydrated phase. It is likely, based on this study, that some or all of the scattering at z = 0.5 is due to the presence of N(2) or MMA(2).

Electrostatic interactions between the ammonium-group and the oxygen atom plane cannot explain the difference in the orientations of MMA(1) and MMA(2). It is possible that the two orientations result from differences in hydration states of the two molecules. However, we do not have sufficient data to determine this.

DMA-vermiculite

Intercalation of the Santa Olalla vermiculite with DMA resulted in a $d(00l)$ = 12.29 Å, which is comparable to the dehydrated structure (Rowland and Weiss, 1961) of 12.5 Å for DMA-montmorillonite at concentrations of 100% CEC. Longer exchange times did not produce a greater exchange.

In DMA-vermiculite as derived from the X-ray analysis, the N site appears to have four possible associated C atoms (C1, C2, and symmetry-related atoms). The more likely arrangement is that DMA molecules are arranged in two orientations throughout the structure: one DMA molecule has a C1–N–C1 angle of 108° and the other DMA molecule has a C2–N–C2 angle of 105° (Table 2). The estimated standard devi-

https://doi.org/10.1346/CCMN.1999.0470310 Published online by Cambridge University Press

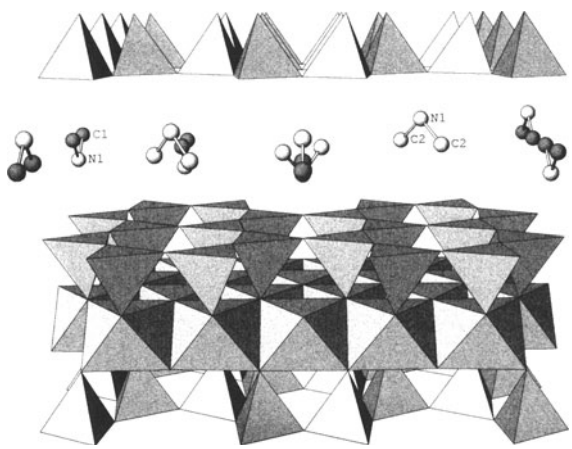

Figure 4. Model structure of the DMA-exchanged vermiculite viewed nearly along the [100] direction. The DMA is represented as "ball and stick", see Figure 1 for details of 2:1 layer.

ations for these C positions may be quite high, because the atomic parameters were not determined by *least-squares*. Thus, these angles represent only approximations. Nonetheless, both values are near the ideal tetrahedral angle of 109.5° and thus support the conclusion that there are two orientations. These angle differences may be related also to the development of H bonds between the basal oxygen atom plane and the H of the NH_2^+ group, where differences in the H bond strength may result in differences in these C–N–C angles.

Both N atoms superpose in the average structure as determined by X-ray analysis, whereas the C atoms do not. This model is "static" and the molecules are in well-defined locations. Figure 4 shows the structure of DMA-vermiculite based on this interpretation of DMA orientations. Although unlikely, this model may be an artifact of the choice of the space group, since the symmetry-related C atoms may be imposed by the mirror plane generated, for example, by Friedel's Law. If this is the case, then the space group is either *C*2 (monoclinic) or *C*1 (triclinic).

Another interpretation of DMA molecular orientation is more dynamic. In this case, C1 and C2 sites are occupied statistically and DMA-molecules are rotating about one C–N axis, as illustrated in Figure 5. This model may explain why the distance of the N atom to the basal oxygen atom plane in DMA-vermiculite is considerably greater than in MMA-vermiculite (Table 3). In addition, differences in distance may be attributed to the different number and strengths of H bonds between MMA and DMA and the basal oxygen atom plane.

The N atom is offset from the central plane of the interlayer by 0.95 Å, and C atoms are at $z = 0.5$ (Table 2). The offset of N and the location of the C atoms produces a zigzag arrangement of DMA in the (001) plane in the static model. In this "chain" [we believe that the term "chain" should be reserved for structural motifs that are linked, but we follow the usage here of Rowland and Weiss (1961)], the plane defined by the C–N–C molecule is perpendicular to the (001) plane. Thus, if DMA-vermiculite may be compared to DMA-montmorillonite (Rowland and Weiss, 1961), our results do not support the model for the 12.5-Å phase of montmorillonite. In that model, the N of the DMA must be located at $z = 0.5$ to produce a zigzag "chain" of DMA in the (001) plane with the plane defined by the C–N–C molecule parallel to the (001) plane. Interestingly, Rowland and Weiss (1961) pre-

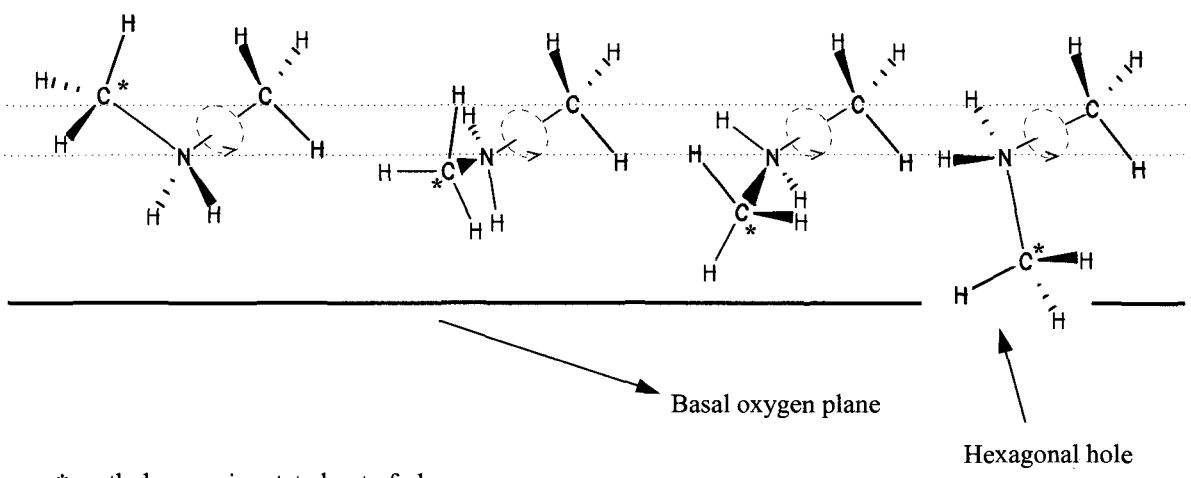

Figure 5. Rotational (dynamic) model for DMA pillars in DMA-exchanged vermiculite, viewed along the (001) plane. In this model, the methyl groups are freely rotating; note the arrow indicating the N–C axis of rotation. The methyl group identified with an asterisk (*) is rotating out-of-plane, as illustrated.

https://doi.org/10.1346/CCMN.1999.0470310 Published online by Cambridge University Press

dicted a zigzag "chain" with the C–N–C axis perpendicular to the (001) plane for the 12.7-Å phase of DMA-montmorillonite, and this "chain" is similar to the one found in vermiculite.

TrMA

In contrast to other examined onium-vermiculites (this study; Vahedi-Faridi and Guggenheim, 1997), TrMA-vermiculite did not show three-dimensional stacking order as indicated by intensity diffuseness parallel to the [001]* direction of $k \neq 3n$ reflections. The minimum pillar height of the TrMA molecule (3.04 Å) is similar in height to the DMA molecule (3.25 Å), where the latter is oriented perpendicular to the basal oxygen atom plane. In contrast, the maximum height (4.54 Å) of the TrMA molecule is close to that of the TMA molecule (4.16 Å, Vahedi-Faridi and Guggenheim, 1997). However, the $d(001)$-value of TrMA-vermiculite lies between that of DMA-vermiculite and TMA-vermiculite (Tables 3 and 4), suggesting that the TrMA molecule is randomly oriented in the interlayer. This randomized orientation seemingly does not have the capability to lock the silicate layers symmetrically, thus leading to random interstratification.

2:1 layer

Comparisons between this study (Tables 4 and 5) and two previous studies using Santa Olalla vermiculite as starting material (Vahedi-Faridi and Guggenheim, 1997, 1999) show that the mean bond lengths for each of the cation sites in the 2:1 layer are nearly identical (MMA, DMA, TMA, TMP for T: 1.654, 1.657, 1.657, 1.660 Å; for M1: 2.082, 2.077, 2.089, 2.075 Å; for M2: 2.081, 2.074, 2.087, 2.074 Å). These values suggest that the chemistry of the 2:1 layer remains constant regardless of the composition of the interlayer. Note also that mean bond lengths of M1 and M2 sites within each sample are identical within estimated standard deviations (Table 4), indicating the lack of octahedral cation ordering in each sample.

However, individual bond lengths and angles do vary significantly within and between coordination units, thereby indicating that each organic molecule substitution affects the 2:1 layer. A small effect is observed for distances involving the apical oxygen atom, O(3), which varies systematically between the four samples, with MMA and TMA-vermiculite being similar with relatively smaller T–O(3) distances and larger M1,M2–O(3) distances, compared to DMA and TMP-vermiculite (MMA, DMA, TMA, TMP: tetrahedron 1.635(5), 1.662(5), 1.631(6), 1.660(3) Å; octahedron M1: 2.095(4), 2.083(4), 2.099(4), 2.084(3) Å; octahedron M2: 2.082(4) and 2.085(4), 2.074(3) and 2.075(4), 2.083(5) and 2.095(4), 2.070(3) and 2.082(2) Å). Octahedral thickness (Table 5) follows the same trend, with MMA and TMA-vermiculites being similar with a thicker octahedral sheet than the other two.

The interaction between the exchanged organic cation and the basal oxygen atom plane should affect the tetrahedral bond distances, and to a lesser extent, the octahedral bond distances. A close approach by the charged organic molecule to a basal oxygen (O_b) atom will result in a weakening of the T–O_b bond (making the distance longer), a strengthening of the T–O3 (apical) bond, and a weakening of M1 or M2 to O3 bonds. Table 3 shows organic cation to basal oxygen atom distances, where MMA more closely approaches the basal oxygen plane than DMA, and TMA more closely approaches the basal oxygen plane than TMP. Comparisons between MMA and DMA show this trend of bond distances (Table 4), as do comparisons between TMA and TMP. Because the geometry of the tetrahedrally-shaped molecules (TMA, TMP) is different from MMA and DMA, these groups should not be compared. The geometrical differences produce a well shielded charge in TMA and TMP, but not in the other cations.

The tetrahedral rotation angle, α, is significantly different for each exchanged vermiculite (Table 5), although the chemical composition of the 2:1 layer is identical for all samples. The tetramethylonium-vermiculites exhibit a much greater tetrahedral rotation than MMA- and DMA-vermiculite. The major difference of these two groups is the association of the positive charge and methyl-group of the pillar to the tetrahedra of the 2:1 layers. For tetramethylonium-vermiculites, this positive charge is shielded by the methyl-groups. In contrast, for MMA- and DMA-vermiculite, there is a more direct interaction between the positively-charged nitrogen ion and the basal oxygen atoms. This interaction may be responsible for the lesser degree of tetrahedral rotation for MMA and DMA-exchanged vermiculite. TMA-vermiculite and MMA-vermiculite have the larger tetrahedral rotation compared to TMP-vermiculite and DMA-vermiculite, respectively. Vahedi-Faridi and Guggenheim (1999) suggested that there will be greater tetrahedral rotation where there is a (relatively small) centrally-located cation within the tetrahedral ring, since there are electrostatic attractions between this cation and the nearest neighbor basal oxygen atoms. Also consistent with this model, the MMA molecule in MMA-vermiculite is centrally located with respect to its tetrahedral ring, and it has a larger α value than DMA-vermiculite. The comparison cannot be extended to include (unexchanged) Llano vermiculite, however, because the partially-occupied interlayer sheet forms hydrogen bonds to the basal oxygen atom plane.

CONCLUSION

This study compares two simple organic molecules (MMA, DMA) with an asymmetric distribution of

https://doi.org/10.1346/CCMN.1999.0470310 Published online by Cambridge University Press

Table 4. Selected calculated bond lengths and angles.

Bond length (Å) and Bond angles (°) of MMA-vermiculite					Bond length (Å) and Bond angles (°) of DMA-vermiculite			
				About T				About T
T–O(1)	1.663(4)	O(1)–O(2)′	2.694(5)	108.5(3)	1.655(3)	O(1)–O(2)′	2.689(5)	108.7(2)
O(2)′	1.656(5)	O(2)	2.689(5)	108.0(3)	1.653(4)	O(2)	2.690(5)	108.6(3)
O(2)	1.661(4)	O(3)	2.712(8)	110.7(3)	1.656(4)	O(3)	2.719(8)	110.1(3)
O(3)	1.635(5)	O(1)–O(2)′	2.692(5)	108.5(3)	1.662(5)	O(2)–O(2)′	2.689(4)	108.7(2)
mean	1.654	O(3)	2.703(7)	110.4(3)	1.657	O(3)	2.724(6)	110.5(2)
		O(2)′–O(3)	2.709(7)	110.6(3)		O(2)′–O(3)	2.720(6)	110.1(2)
		mean	2.700	mean 109.5		mean	2.705	mean 109.5
				About M(1)				About M(1)
		Shared				shared		
M(1)–O(3) × 4	2.095(4)	O(3)–O(3) × 2	2.829(6)	85.0(2)	2.083(4)	O(3)–O(3) × 2	2.802(6)	84.5(2)
OH × 2	2.056(5)	OH × 4	2.766(7)	83.6(2)	2.065(4)	OH × 4	2.757(7)	83.3(1)
mean	2.082	mean	2.798		2.077	mean	2.780	
		unshared				unshared		
		O(3)–O(3) × 2	3.090(5)	95.0(2)		O(3)–O(3) × 2	3.083(5)	95.5(2)
		OH × 4	3.094(5)	95.4(2)		OH × 4	3.098(4)	96.7(1)
		mean	3.092			mean	3.091	
				About M(2)				About M(2)
		shared				shared		
M(2)–O(3) × 2	2.082(4)	O(3)–O(3)	2.829(6)	85.6(2)	2.074(3)	O(3)–O(3)	2.802(6)	84.9(2)
O(3)′×2	2.085(4)	O(3)′ × 2	2.815(6)	85.0(2)	2.075(4)	O(3)′ × 2	2.789(6)	84.5(2)
OH × 2	2.075(4)	OH–O(3)′ × 2	2.766(7)	83.4(2)	2.073(4)	OH–O(3)′ × 2	2.757(7)	83.3(2)
mean	2.081	OH	2.727(9)	82.2(2)	2.074	OH	2.726(7)	82.2(2)
		mean	2.784			mean	2.769	
		unshared				unshared		
		O(3)–O(3)′ × 2	3.091(5)	95.8(2)		O(3)–O(3)′ × 2	3.093(4)	96.4(2)
		OH × 2	3.092(4)	96.1(2)		OH × 2	3.093(4)	96.4(2)
		OH–O(3)′ × 2	3.088(5)	95.8(2)		OH–O(3)′ × 2	3.077(4)	95.8(2)
		mean	3.090			mean	3.088	

Bond length (Å) and Bond angles (°) of TMA-vermiculite					Bond length (Å) and Bond angles (°) of TMP-vermiculite			
				About T				About T
T–O(1)	1.664(4)	O(1)–O(2)′	2.698(5)	108.3(3)	1.658(2)	O(1)–O(2)′	2.693(4)	108.6(2)
O(2)′	1.664(5)	O(2)	2.697(5)	108.0(2)	1.658(3)	O(2)	2.694(4)	108.5(2)
O(2)	1.670(4)	O(3)	2.707(8)	110.5(3)	1.662(3)	O(3)	2.723(5)	110.3(2)
O(3)	1.631(6)	O(2)–O(2)′	2.697(5)	108.0(3)	1.660(3)	O(2)–O(2)′	2.693(3)	108.5(2)
mean	1.657	O(3)	2.722(2)	111.1(2)	1.660	O(3)	2.725(4)	110.5(2)
		O(2)′–O(3)	2.713(7)	110.8(2)		O(2)′–O(3)	2.728(4)	110.5(1)
		mean	2.706	mean 109.5		mean	2.709	mean 109.5
				About M(1)				About M(1)
		shared				shared		
M(1)–O(3) × 4	2.099(4)	O(3)–O(3) × 2	2.838(7)	85.1(2)	2.084(3)	O(3)–O(3) × 2	2.797(4)	84.3(1)
OH × 2	2.070(6)	OH × 4	2.792(8)	84.1(2)	2.059(4)	OH × 4	2.757(4)	83.4(1)
mean	2.089	mean	2.815		2.075	mean	2.777	
		unshared				unshared		
		O(3)–O(3) × 2	3.093(5)	94.9(2)		O(3)–O(3) × 2	3.089(4)	95.7(1)
		OH × 4	3.098(4)	96.0(2)		OH × 4	3.092(4)	96.6(1)
		mean	3.096			mean	3.091	
				About M(2)				About M(2)
		shared				shared		
M(2)–O(3) × 2	2.083(5)	O(3)–O(3)	2.838(7)	85.9(2)	2.070(3)	O(3)–O(3)	2.797(4)	85.0(1)
O(3)′×2	2.095(4)	O(3)′ × 2	2.832(7)	85.3(2)	2.082(2)	O(3)′ × 2	2.795(4)	84.6(1)
OH × 2	2.082(5)	OH–O(3)′ × 2	2.792(8)	83.9(2)	2.069(3)	OH–O(3)′ × 2	2.757(4)	83.2(1)
mean	2.087	OH	2.747(9)	82.6(2)	2.074	OH	2.713(6)	82.0(1)
		mean	2.802			mean	2.766	
		unshared				unshared		
		O(3)–O(3)′ × 2	3.089(5)	95.4(2)		O(3)–O(3)′ × 2	3.088(4)	96.1(1)
		OH × 2	3.090(4)	95.9(2)		OH × 2	3.089(3)	96.5(1)
		OH–O(3)′ × 2	3.088(5)	95.4(2)		OH–O(3)′ × 2	3.086(4)	96.0(1)
		mean	3.089			mean	3.088	

https://doi.org/10.1346/CCMN.1999.0470310 Published online by Cambridge University Press

Table 5. Calculated structural parameters for methyl-onium-vermiculites.

Parameter	TMP-vermiculite	TMA-vermiculite	DMA-vermiculite	MMA-vermiculite
$\alpha(^\circ)$[1]	6.75	7.1	5.8	6.1
$\Psi(^\circ)$[2]	59.57 M(1)	59.17 M(1)	59.52 M(1)	59.42 M(1)
	59.55 M(2)	59.10 M(2)	59.47 M(2)	59.40 M(2)
$\tau_{tet}(^\circ)$[3]	110.4	110.7	110.2	110.6
Sheet thickness[4]				
octahedral (Å)	2.102	2.142	2.107	2.119
tetrahedral (Å)	2.264	2.125	2.254	2.251
Interlayer separation (Å)	7.764	6.852	5.677	5.189
ΔZ_{ave} (Å)[5]	0.004	0.014	0	0.012
β_{ideal} (°)[6]	97.06	97.53	98.26	98.59

[1] α = 1/2[120° − mean O_b–O_b–O_b angle].
[2] Ψ = $\cos^{-1}$[(oct. thickness)/(2(M–O)$_{ave}$)].
[3] τ = mean O_b–T–O_a.
[4] Tetrahedral thickness includes OH.
[5] Δz_{ave} = Basal oxygen corrugation.
[6] β_{ideal} = 180° − $\cos^{-1}$[a/3c].

charge. In MMA-vermiculite, there are at least two orientations for the MMA molecule. In one orientation, the N of the MMA molecule is associated with the hexagonal ring to offset the layer charge originating from Al for Si tetrahedral substitutions. In contrast, a second MMA orientation has the source of the charge on the molecule, N, exactly between the adjacent 2:1 layers [if this orientation is dynamic, then there are multiple orientations, although this molecule presumably remains parallel to the (001) plane]. This is the first reported case for a 2:1 layer phyllosilicate where the organic molecule is found exactly between the layers, much like inorganic interlayer cations. The two orientations of MMA molecules may be related to different hydration states of the molecules, but because any interlayer water is randomly distributed between the layers, X-ray data alone cannot be used to locate H_2O molecules. DMA-vermiculite shows two crystallographically unique DMA molecules, where the C–N–C planes differ in orientation, although both planes are normal to the (001).

Mean bond lengths of coordination polyhedra in the 2:1 layer for MMA, DMA, TMA, and TMP-exchanged vermiculites indicate that the respective polyhedra are chemically identical, but individual bond lengths differ significantly. MMA and DMA-exchanged vermiculites *vs.* TMA and TMP-exchanged vermiculites show different bond-length systematics in the polyhedra of the 2:1 layer because of differences in the geometries of the organic molecule. Additional evidence for interactions between the organic molecule and the silicate layer is indicated by the different tetrahedral rotation angles of the vermiculite structures. Clearly, the organic molecule has an important affect on the silicate layer substrate.

This study does not address two important features of these organo-vermiculite structures: (1) the number, position, and orientation of the H_2O molecules in the interlayer and (2) the extent that hydrogen bonds may play in the bonding between the organic cations and basal-oxygen atom planes. Further work is necessary to develop a better understanding of these features.

ACKNOWLEDGMENTS

We thank P. Slade, C.S.I.R.O., Adelaide, Australia, for providing samples of vermiculite that made this study possible, M. Wahle, University of Illinois at Chicago, for locating a suitable DMA-vermiculite crystal, and R. Ferrell and especially an anonymous reviewer for excellent suggestions in the review process. Partial support of this work was made possible by the donors of The Petroleum Research Fund, administered by the American Chemical Society, under grant PRF-32858-AC5.

REFERENCES

Barrer, R.M. (1989) Shape-selective sorbents based on clay minerals: A review. *Clays and Clay Minerals*, **37,** 385–395.

Barrer, R.M. and McLeod, D.M. (1955) Activation of montmorillonite by ion exchange and sorption complexes of tetra-alkyl ammonium montmorillonites. *Transactions of the Faraday Society*, **50,** 1290–1300.

Barrer, R.M. and Millington, A.D. (1967) Sorption and intracrystalline porosity in organo-clays. *Journal of Colloid Interface Science*, **25,** 359–372.

Barrer, R.M. and Reay, J.S.S. (1957) Sorption and intercalation by methylammonium montmorillonites. *Transactions of the Faraday Society*, **53,** 1253–1261.

Cromer, D.T. and Mann, J.B. (1968) X-ray scattering factors computed from numerical Hartree-Fock wave functions. *Acta Crystallographica*, **A24,** 321–324.

de la Calle, C., Suquet, H., and Pezerat, H. (1985) Vermiculites hydratees a une couche. *Clay Minerals*, **20,** 221–230.

Diamond, S. and Kinter, E.B. (1961) Characterization of montmorillonite saturated with short chain amine cations. *Clays and Clay Minerals*, **10,** 163–173.

Ladd, M.F.C. and Palmer, R.A. (1977) *Structure Determination by X-ray Crystallography.* Plenum Press, New York, 393 pp.

Luque, F.J., Rodas, M., and Doval, M. (1985) Mineralogia y genesis de los yacimientos de vermiculite de Ojen. *Boletin Sociedad Española de Mineralogíe*, **8,** 229–238.

Norrish, K. (1973) Factors in the weathering of mica to vermiculite. In *Proceedings of the International Clay Conference, Madrid: 1972*, J.M. Serratosa, ed., Division de Ciencias, CSIC, Madrid, 417–432.

Rowland, R.A. and Weiss, E.J. (1961) Bentonite-methylamine complexes. *Clays and Clay Minerals*, **10,** 460–468.

Sales, K.D. (1987) Atomic scattering factors for mixed atom sites. *Acta Crystallographica*, **A43,** 42–44.

Siemens (1990) SHELXTL PLUS 4.0. Siemens Analytical X-ray Instruments, Inc., Madison, Wisconsin.

Slade, P.G. and Stone P.A. (1984) Three-dimensional order and the structure of aniline-vermiculite. *Clays and Clay Minerals*, **32,** 223–226.

Theng, B.K.G., Greenland, D.J., and Quirk, J.P. (1967) Adsorption of alkylammonium cations by montmorillonite. *Clay Minerals*, **7,** 1–17.

Vahedi-Faridi, A. and Guggenheim, S. (1997) Crystal structure of TMA-exchanged vermiculite. *Clays and Clay Minerals*, **45,** 859–866.

Vahedi-Faridi, A. and Guggenheim, S. (1999) Structural study of TMP-exchanged vermiculite. *Clays and Clay Minerals*, **47,** 219–225.

Williams, G.D., Skipper, N.T., Smalley, M.V., Soper, A.K., and King, S.M. (1996) Structure of alkylammonium solutions in vermiculite clays. *Faraday Discussions*, **104,** 295–306.

(Received 30 March 1998; accepted 4 December 1998; Ms. 98-040)